Journal of Electronic Materials (2021) 50:6929–6940
https://doi.org/10.1007/s11664-021-09242-7

ORIGINAL RESEARCH ARTICLE

Electroanalytical Determination of Acetaminophen Using a Polymerised Carbon Nanotube Based Sensor

M. M. Charithra[1] · J. G. Manjunatha[1]

Received: 13 May 2021 / Accepted: 14 September 2021 / Published online: 28 September 2021

Abstract

In this paper, acetaminophen (AP), typically consumed as a painkiller, was sensitively detected using an electrochemical sensor through cyclic voltammetry. Therefore, special attention focused on fabricating a sensitive voltammetric sensor based on cetrimide (CA) incorporated on a poly oxalic acid modified carbon nanotube paste electrode (POAMCNTPE). The topographical features and electrochemical characterisations of unmodified and modified electrodes were compared using a variable pressure scanning electron microscope (VP-SEM) and electrochemical impedance spectroscopy (EIS). The scan rate study reveals that the redox reaction of the AP at the surface of the modified electrode was controlled by diffusion. The detection limit (DL) of 1.50×10^{-8} M and quantification limit (QL) of 5.02×10^{-8} M was gained by utilising differential pulse voltammetry (DPV). The constructed electrochemical sensor displayed acceptable repeatability, excellent stability, and adequate reproducibility. The prepared sensor exhibited an outstanding selectivity to detect the AP in the presence of dopamine (DA) and folic acid (FA). The practicability of the proposed electrode was examined to be successful towards the quantification of AP in both pharmaceutical and biological samples.

✉ J. G. Manjunatha
manju1853@gmail.com

[1] Department of Chemistry, FMKMC College, Mangalore University Constituent College, Madikeri, Karnataka, India

Graphic Abstract

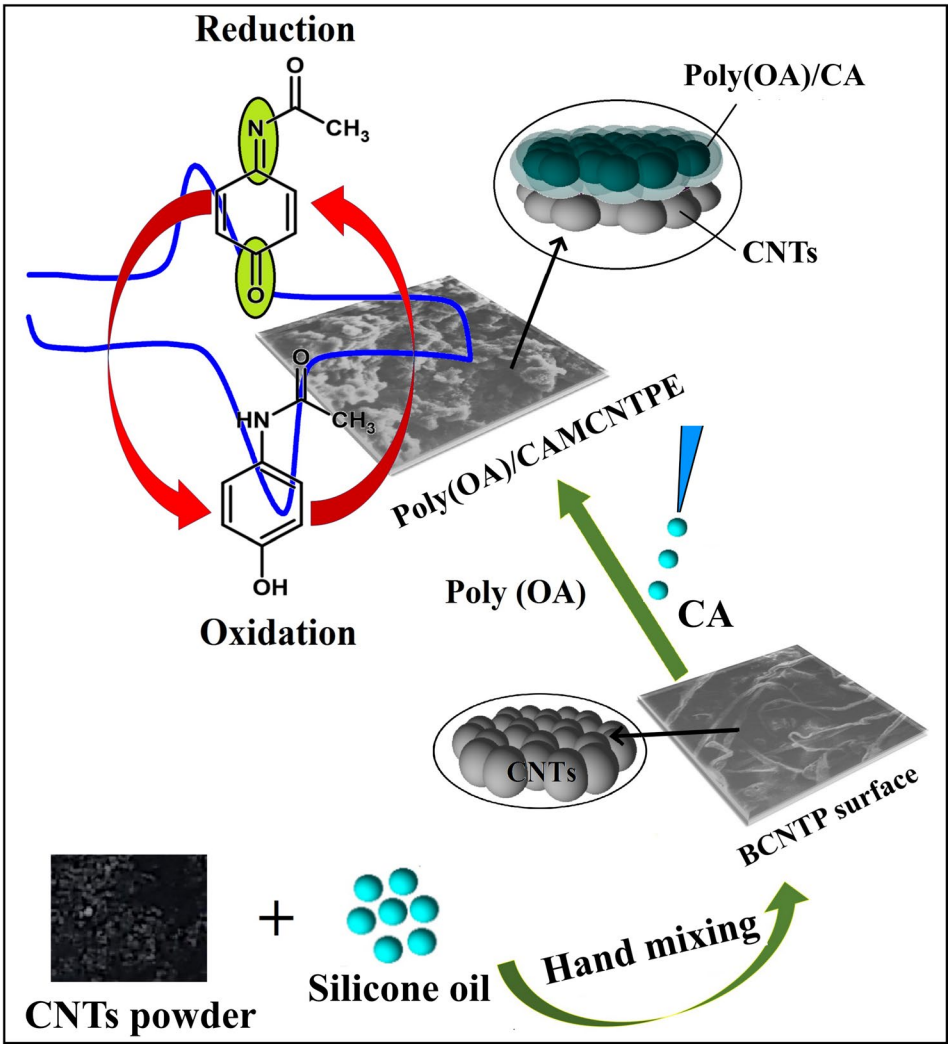

Keywords Acetaminophen · carbon nanotube paste electrode · dopamine · electropolymerisation · immobilization

Introduction

Drugs are tools suited for a particular therapeutic action; they cure diseases and improve health. Analgesic drugs or painkillers are a major class of drugs and are used worldwide. Acetaminophen (AP), also known as paracetamol, is an acetylated aromatic amide, utilised as an analgesic and antipyretic agent. It is used as an analgesic agent to alleviate pain associated with all the parts of the body. AP is used as an antipyretic agent to reduce fever from a bacterial infection.[1–3] AP is a non-carcinogenic and anti-inflammatory non-steroidal drug and provides the safest option available for aspirin-sensitive patients.[4–6] AP generally has no adverse side effects because it is fully digested into inactive metabolites that can be readily excreted through urine.[7] However, overdose or chronic use of AP leads to a toxic metabolite accumulation resulting in skin rashes and damage to the pancreas, liver, and kidneys.[8–10] To prevent disease, AP analysis is important, thus it is very significant to develop a simple, rapid, low-cost electro-analytical method for the detection of AP.

To date, the literature has reported several techniques used for the determination of AP.[11] These consist of capillary electrophoresis,[12] chemiluminescence,[13] high-performance liquid chromatography,[14,15] infrared spectroscopy,[16] batch injection analysis,[17] liquid chromatography,[18–20] titrimetric measurement,[21,22] spectrometry.[23,24] These techniques offer high sensitivity, good selection, and accurate application but are limited by their complex applications, including technical challenges of use, time-consuming procedures, skilled

technicians, and high-cost instruments. Among these, some techniques are less suitable to determine AP. Hence, electrochemical methods are the most substantial technique in the field of analytical chemistry.[25–27] However, voltammetric techniques represent one of the most straightforward and most sensitive techniques among the existing electrochemical methods and measure both the current and potential.[28–32] Cyclic voltammetry (CV) is one of the main classes of the voltammetric technique.[33–38] Thus, CV approaches provide an easy, rapid, and selective detection of an analyte with low-cost and environmentally friendly equipment.[39]

Carbon nanotubes (CNTs) are molecular tubes possessing excellent characteristics of graphite. CNTs have gained significant recognition in developing electrochemical sensors owing to their physical and chemical properties.[40–42] The literature reviewed reveals that CNT-based electrochemical sensors provide benefits such as enhanced electron transfer rates, surface fouling avoidance, high sensitivity, rapid response time, and electrocatalytic activity towards various compounds.[43–45] Therefore, CNTs are valuable candidates for the construction of an electrochemical sensor.[46] To modify CNTs, the method of electropolymerisation and immobilization was implemented to enhance the electrocatalytic activity of the fabricated sensor. Electropolymerisation is a method for regulating the number of cycles and potential applied in an electrode, in which a certain thickness of the polymer film is achieved.[47] Surfactants are active on the surface and are amphiphilic in nature. They can improve the rate of electron transfer due to interface adsorption. Hence, surfactants are useful in electrochemistry.[48–50]

The present study reports the fabrication of cetrimide (CA) incorporated on a poly oxalic acid (POA) modified carbon nanotube paste electrode (MCNTPE). The CA/POAMCNTPE provides an exceptional electrocatalyst property towards the oxidation of AP via CV. The viability of the constructed sensor was evaluated by detecting the AP in the tablet and blood serum samples. A literature review revealed that detecting AP with CA/POAMCNTPE using CV has not been reported until now. Finally, a low-cost, simple, rapid, and high sensitivity voltammetric method was developed to detect AP.

Experimental Analysis

Instrumentation

Electrochemical investigations were performed by utilising an electrochemical workstation model CHI-6038E (CH Instruments, USA), interfaced to a personal computer for data acquisition and equipped with a tri-electrode cell. The electrolytic cell had a platinum wire as a counter electrode, a saturated calomel electrode functioning as a reference electrode, and a bare carbon nanotube paste electrode (BCNTPE) or CA/POAMCNTPE as a working probe. A VITSIL-VBSD/VBDD water distillation system was used to acquire the distilled water. The variable pressure scanning electron microscope (VP-SEM) was obtained from Vijnana Bhavan, University of Mysore, Manasagangothri (India). The digital pH meter model EQ-610 was employed to prepare the solution with the appropriate pH for the experiment.

Reagents and Chemicals

Sodium dihydrogen phosphate ($NaH_2PO_4.H_2O$, 99.8%), disodium hydrogen phosphate ($Na_2HPO_4.H_2O$, 99%), and CA (99.8%) were purchased from HiMedia Laboratories, Bangalore. AP (99%) was received from Tokyo Chemical Industry Co. Ltd. (Japan). Silicone oil was purchased from Nice Chemicals, India. CNTs were acquired from Sisco Research Laboratories Pvt. Ltd. Mumbai, Maharastra (OD: 30–50 nm and length: 10–30 µm). OA (99.5%), dopamine (DA) (99%), and folic acid (FA) (99%) were obtained from Molychem, India. The highest possible analytical quality chemicals were used in this whole work. The stock solutions of 25×10^{-4} M AP, DA, CA, OA were made using distilled water. A 0.2 M phosphate buffer solution (PBS) was prepared by mixing the appropriate ratio of $NaH_2PO_4{\cdot}H_2O$, $Na_2HPO_4{\cdot}H_2O$. PBS serves as a supporting electrolyte. All voltammetric measurements were carried out at laboratory temperature (25 ± 1°C).

Fabrication of CA/POAMCNTPE

The initial step in the fabrication of CA/POAMCNTPE was BCNTPE preparation. Thus, in an agate mortar with a composition of 60:40 CNTs powder and silicone oil was ground for about 15 min in an agate mortar with a pestle to obtain a homogenous paste. Then, the paste was put into the cavity at the bottom of the Teflon tube and smoothed on a weighing paper. A copper wire connected to the other end of the Teflon tube provided the electrical contact. Hence, BCNTPE was ready for further modification. Electrochemical polymerization of OA on the surface of BCNTPE was carried out using CV. After the electropolymerisation, the electrode was subjected to immobilization of 10 µL of CA for about 5 min at room temperature. After 5 min, the electrode was thoroughly rinsed with double-distilled water. The obtained electrode was labeled as CA/POAMCNTPE and used for further electrochemical analysis.

Results and Discussion

Electrochemical Polymerization of OA on BCNTPE

Electropolymerization is an important factor affecting the voltammetric signal of the targeted analyte. Thus, cyclic voltammograms (CVs) were documented for 1×10^{-4} M OA in 0.2 M supporting electrolyte (pH 7.0) with a scan rate of 0.1 V s^{-1} between a potential window of − 0.7 V to 1.3 V (Fig. 1) for 20 multiple segments. As can be seen from the CVs, the polymer layer increased with increasing cycles signifying that electropolymerization of OA was successfully achieved. Thus, we can conclude that an increase in peak current on successive scans indicates the growth of conducting polymeric film of OA on BCNTPE. The mechanism of electropolymerisation of OA has been already reported.[51] The mechanism of polymerisation of OA involves free-radical formation. The produced free-radical of OA is attached to the electrode consisting of unpaired electrons of carbon. Then, the OA molecules are attached to the already attached OA molecule continuously to form a polymer chain through polymerisation.

Morphological Studies of BCNTPE and CA/POAMCNTPE

VP-SEM can efficiently convey the surface morphological characteristics of the constructed BCNTPE and CA/POAMCNTPE. Figure 2a, b represents the VP-SEM image of BCNTPE and CA/POAMCNTPE, respectively. The VP-SEM images show a clear differentiation between the BCNTPE and CA/POAMCNTPE surface morphology. As seen from its surface, BCNTPE showed rough morphology with a network-like structure of carbon nanotubes. The inset of Fig. 2a reveals the tubes of the carbon. VP-SEM image of CA/POAMCNTPE shown in Fig. 2b shows the smooth surface morphology with a modifier spread over the CNTs, as shown in the inset of Fig. 2b. Thus, distinguishing between the VP-SEM images of BCNTPE and CA/POAMCNTPE provides evidence of the successful implementation of the fabrication of CA/POAMCNTPE.

Electrochemical Characterisation of the Proposed Electrodes

With the benefit of the redox probe K_4 [Fe (CN_6)], CV is an important approach to prove the electrodeposited surface-active layer of the modifier on the BCNTPE. Thus, CVs (Fig. 3) were documented for the 1×10^{-3} M K_4 [Fe (CN_6)] solution containing 0.2 M KCl as a supporting electrolyte at a scan rate of 0.1 V s^{-1} on the surface of the BCNTPE (curve a) and CA/POAMCNTPE (curve b). As can be observed from the CV profile, the magnitude of the peak current was intensified by the CA/POAMCNTPE compared to the BCNTPE; therefore, we can ascertain that the bare electrode with the modifier demonstrated an excellent electrocatalytic feature. The surface-active area of the electrode was predicted by utilising the Randles–Sevcik equation (Eq. 1) as follows,

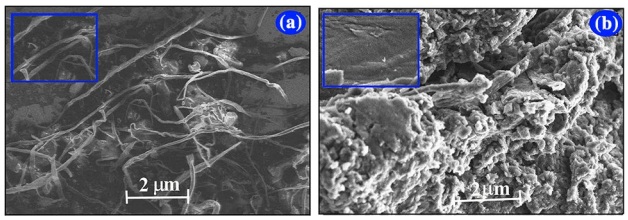

Fig. 2 VP-SEM photograph of the BCNTPE (a) and CA/POAMCNTPE (b).

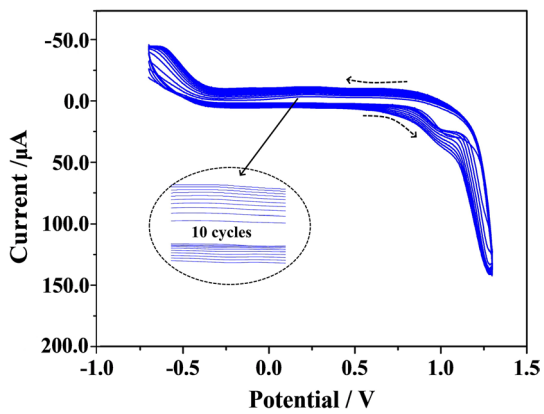

Fig. 1 CVs for electropolymerisation of OA on the surface of BCNTPE in 0.2 supporting electrolyte (pH 7.0) at 0.1 V s^{-1} sweep rate.

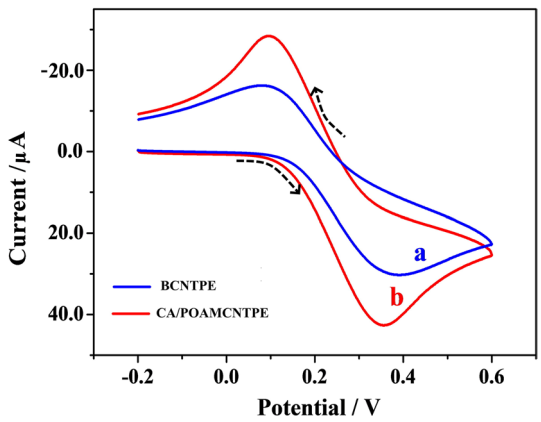

Fig. 3 CVs documented for 1×10^{-3} K_4 [Fe (CN_6)] in 0.2 M KCl as supporting electrolyte at a scan rate of 0.1 V s^{-1} on the surface of the bare (curve a) and modified electrode (curve b).

$$I_{pa} = 2.69 \times 10^5 n^{3/2} A D^{1/2} C v^{1/2} \quad (1)$$

where v is the scan rate, C is the concentration of the solution, n is the number of electrons transferred, A is the surface-active area, D is the diffusion coefficient, I_{pa} is the anodic peak current.[52] The surface-active area 0.04 cm^2 and 0.05 cm^2 for unmodified and modified electrodes were predicted from the above Eq. 1 and hence the larger area of the modified electrode shows that the fabricated electrode has a larger surface-active area and faster electron transfer than the unmodified electrode.

Electrochemical Impedance Spectroscopy (EIS) Study

EIS is a beneficial technique to monitor the interface properties of the surface-modified electrode. EIS study of the proposed electrode was performed using 1×10^{-3} M K_4 [Fe (CN_6)] as a redox probe in 0.1 M KCl as a supporting electrolyte. The spectrum obtained from the EIS study is known as the Nyquist plot involving the semicircular part that denotes electron transfer resistance, and a linear portion represents the diffusion limiting process. The documented Nyquist plot for unmodified (curve b) and modified (curve a) electrodes is displayed in Fig. 4. As inferred from the EIS spectra, the semicircle of the CA/POAMCNTPE was much smaller than the unmodified electrode. The small semicircle proves that the electron transfer at the CA/POAMCNTPE was easier than the unmodified electrode. From the fitted Randles equivalent circuit, the R_{ct} value for the modified electrode and unmodified electrode was 232 Ω and 396 Ω, respectively. The lower R_{ct} value obtained for the CA/POAMCNTPE indicates that the modified electrode has higher conductivity.

Investigation of Voltammetric Response of AP at CA/POAMCNTPE

To compare the voltammetric response of AP between the BCNTPE and CA/POAMCNTPE, the electrochemical behaviour of 1×10^{-4} M AP at BCNTPE and CA/POAMCNTPE in 0.2 M supporting electrolyte (pH 7.0) at a sweep rate of 0.1 V s^{-1} was inspected using CV. As demonstrated in Fig. 5, in the absence of AP (curve a) at CA/POAMCNTPE, a peak was not observed but the voltammetric signal of AP at BCNTPE (curve b) showed a weak current sensitivity (23.3 µA) due to slow electron transfer. However, CA/POAMCNTPE (curve c) shows an enhanced redox current sensitivity (178.9 µA) with E_{pa} 0.361 V for AP. Hence, the MCNTPE effectively boosted the electro-oxidation of AP. The redox peak currents at MCNTPE are higher than the BCNTPE, and the cathodic and anodic potential difference (ΔE_{pa}) is 0.160 V and the redox peak current ratio $I_{pc}/I_{pa} \approx 1$. From this, it is clear that the AP shows a quasi-reversible redox performance.[53]

Study of pH Effect

The hydrogen ion concentration, or pH, of the supporting electrolyte disrupts the redox reaction of the target analyte by swinging the redox potential to positive or negative values. Therefore, an ideal pH is necessary to maximise the sensitivity of the peak current. CVs revealed (Fig. 6a) the impact of pH on the redox reaction of AP at CA/POAMCNTPE in the range 6.0 to 7.5 and showed that the E_{pa} shifted to a side that became more negative with the increase in pH value. The graphical interpretation shows that the peak currents improved considerably with an increase in pH of 7.0 and decreased when the pH was above or below this level. Thus, the supporting electrolyte with pH of 7.0 was

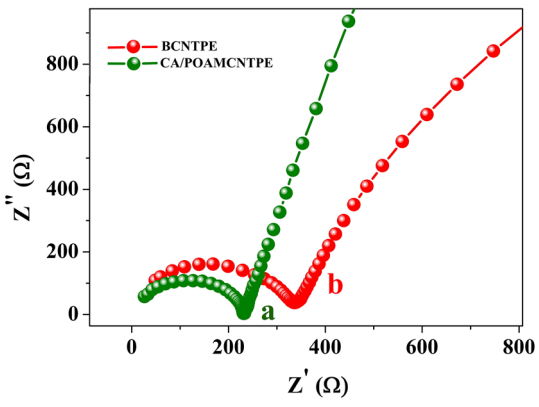

Fig. 4 EIS spectra for modified electrode (a) and unmodified electrode (b).

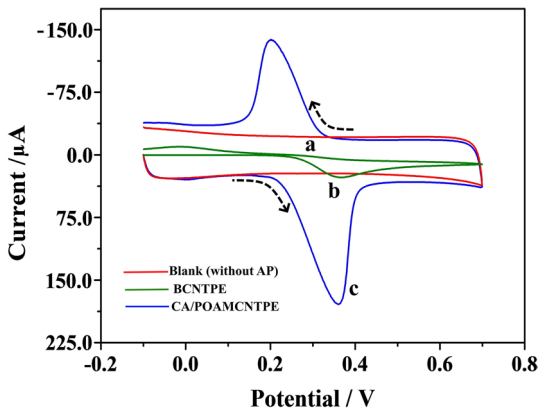

Fig. 5 CVs documented for AP solution using BCNTPE (curve b), CA/POAMCNTPE (curve c) and in the absence of AP (curve a) in 0.2 M supporting electrolyte (pH 7.0).

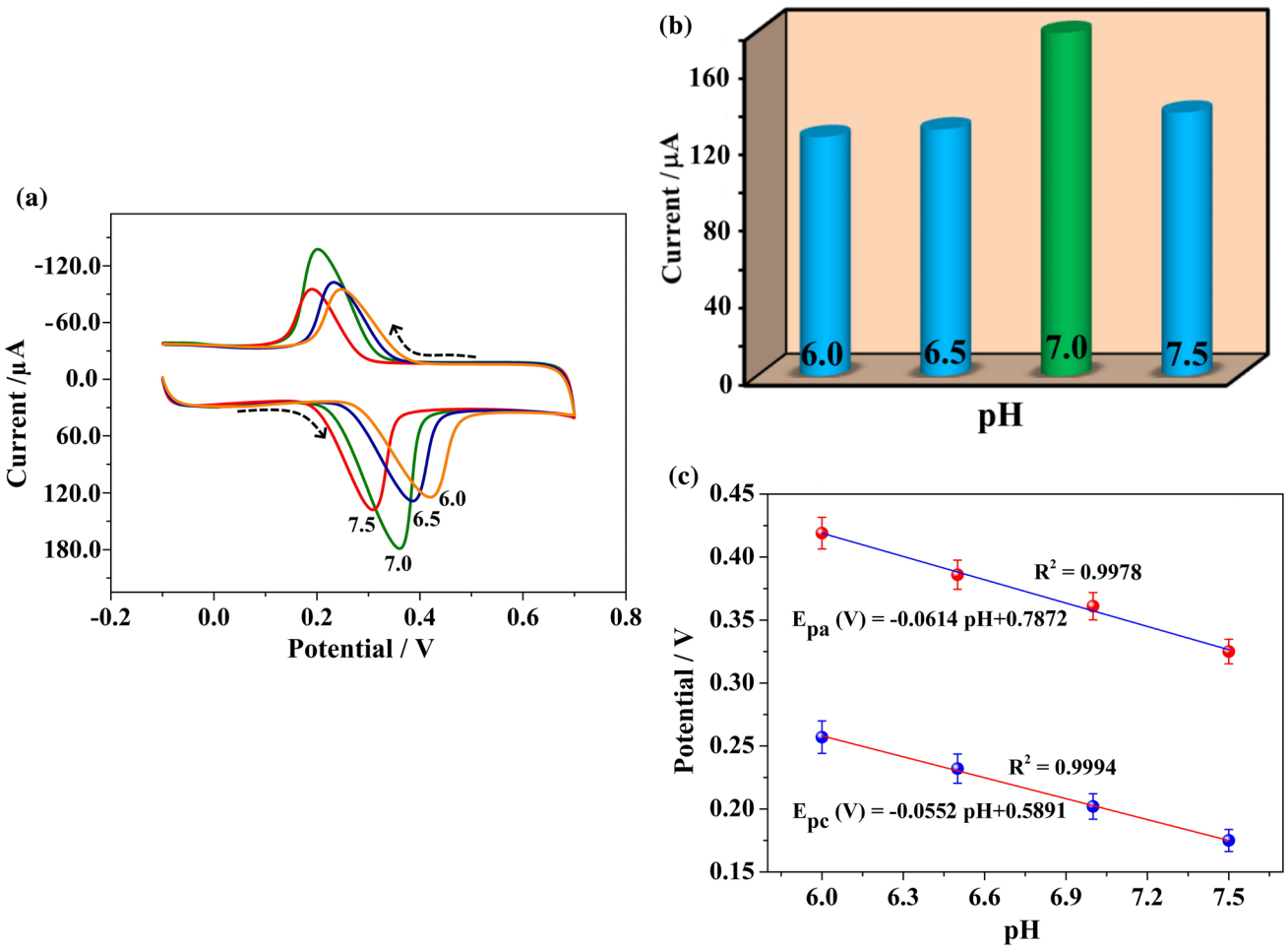

Fig. 6 (a) CVs for 1×10^{-4} M AP utilising the CA/POAMCNTPE at different pH values (6.0–7.5), (b) graph of I_{pa} versus pH, (c) dependence of oxidation and reduction potential on pH.

designated as the optimal pH. The graphical diagram of E_{pa} and E_{pc} against pH (Fig. 6c) shows that the potential depends linearly on the pH. The linear regression equation is represented in the following Eqs. 2 and 3,

$$E_{pa}(\mathrm{V}) = -0.0614(\mathrm{pH}) + 0.7872\left(R^2 = 0.9978\right) \quad (2)$$

$$E_{pc}(\mathrm{V}) = -0.0552(\mathrm{pH}) + 0.5891\left(R^2 = 0.9994\right) \quad (3)$$

Using the slopes acquired from Eqs. 2 and 3, the ratio of protons and electrons participating in the redox reaction of AP can be estimated from the following Eq. 4,

$$dE_{pa}/d_{pH} = 2.303mRT/nF \quad (4)$$

where m is the number of protons and n is the number of electrons.[54] The calculated m/n ratio was 1.038 and 0.93 for oxidation and reduction reaction of AP, respectively. These results show that quantities of protons and electrons participating are nearly equal. Hence, AP successfully undergoes two-electron/two-proton redox reactions on the surface of the CA/POAMCNTPE. The mechanism of electro-oxidation of AP is shown in Scheme 1

Impact of Potential Scan Rate

The electron transfer functionality of the proposed modified electrode can be understood by evaluating the scan rate. The CVs (Fig. 7a) demonstrate the voltammetric response of AP with a scan rate from 0.05 V s^{-1} to 0.2 V s^{-1} at CA/POAMCNTPE in a 0.2 M supporting electrolyte (pH 7.0). As noted from the CVs, the AP anodic signal has increased and moved towards the positive potential with the increase in scan rate revealing the quasi-reversible nature. The graphical plot of I_{pa} and I_{pc} versus $v^{1/2}$ (Fig. 7b) is linear in the relation, and the equation is as follows in Eqs. 5 and 6,

$$I_{pa}(\mu A) = 0.0015v^{1/2}/\left(Vs^{-1}\right)^{1/2} - 81.2643\ \left(R^2 = 0.9988\right) \quad (5)$$

$$I_{pc}(\mu A) = -0.0013v^{1/2}/\left(Vs^{-1}\right)^{1/2} + 114.0\left(R^2 = 0.9957\right). \quad (6)$$

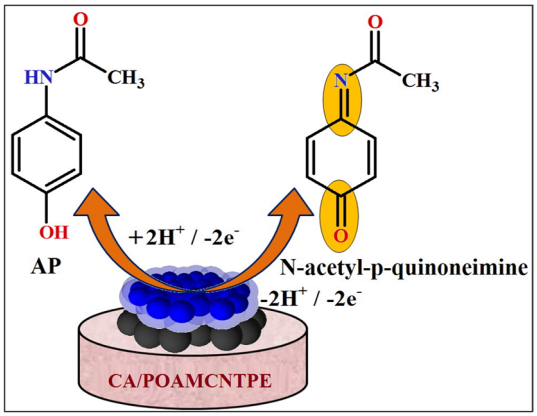

Scheme 1 Redox reaction of AP at CA/POAMCNTPE.

This shows that the redox process of AP was controlled by diffusion. The constructed graph of log I_{pa} versus log v (Fig. 7c) gives the linear association, and the linear segment equation is as follows in Eq. 7,

$$I_{pa}(\mu A) = 0.6367\ \log\left(v/Vs^{-1}\right) + 1.3929\left(R^2 = 0.9994\right). \quad (7)$$

The best slope value from the graph is 0.63, which is near to the hypothetical value of 0.5 and strongly implies that the redox process of AP is controlled by diffusion.[55] Furthermore, the graph of potential against the logarithm of the scan rate (Fig. 7d) was constructed and the linear segment equation is displayed in the following Eqs. 8 and 9,

$$E_{pa}(V) = 0.1163\ \log\ \left(v/Vs^{-1}\right) + 0.0885\left(R^2 = 0.9977\right) \quad (8)$$

$$E_{pc}(V) = -0.0486\ \log\ \left(v/Vs^{-1}\right) + 0.5112\left(R^2 = -0.9868\right). \quad (9)$$

The best slope of the above Eqs. 8 and 9 is equal to the following Eqs. 10 and 11

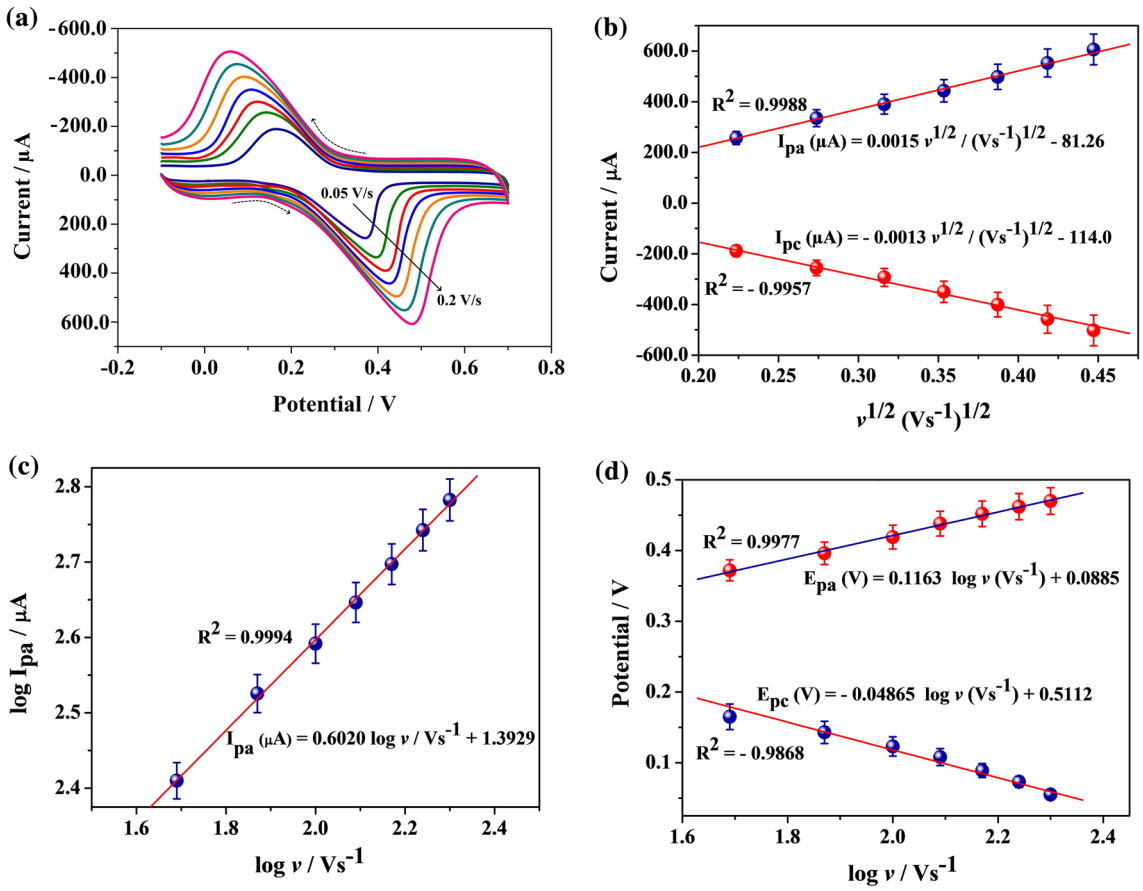

Fig. 7 (a) CVs at various sweep rates (0.05–0.2 V s^{-1}) of 1×10^{-4} M AP using CA/POAMCNTPE in a 0.2 M supporting electrolyte (pH 7.0), (b) Linear relationship between the peak current and the square root of the sweep rate, (c) Plot of the logarithm of peak current against the logarithm of sweep rate, (d) Graph of potential against logarithm of sweep rate

$$E_{pa} = 2.303RT/(1-\alpha)nF \quad (10)$$

$$E_{pc} = -2.303RT/\alpha nF \quad (11)$$

where n specifies transferred electrons, α is a charge transfer coefficient and others have their usual meanings.[56] The estimated number of electrons transferred during the reaction at the modified sensor was two by using the above Eqs. 10 and 11. Therefore, the redox reaction of the AP takes place by losing the two electrons at the modified sensor.

Analytical Curve and Figure of Merit

The objective of this method was to detect a low concentration of the target analyte using the proposed sensor. Thus, detection limit (DL) and quantification limit (QL) are statistical standards for measuring the efficiency of the sensor. As a comparison, the DL was estimated by employing both CV and differential pulse voltammetry (DPV). Therefore, CVs (Fig. 8a) and differential pulse voltammograms (DPVs, Fig. 8c) were documented for the AP concentration range from 2.0 µM to 50 µM at CA/POAMCNTPE under the ideal experimental conditions. The calibration curve was plotted for CV response (Fig. 8b) as well as DPV response (Fig. 8d). The linear relationship between the AP concentration and peak current occurred as intended using either technique. As can be seen from Fig. 8b, two linear ranges appeared in the range of 2.0–10 µM and 15.0–50 µM for the CV response, and the linear segment equation is expressed as follows in Eqs. 12 and 13,

$$I_{pa}(\mu A) = 38.512 + 2.142\ C(M)\ \left(R^2 = 0.9978\right) \quad (12)$$

$$I_{pa}(\mu A) = 40.850 + 1.703\ C\ (M)\ \left(R^2 = 0.9978\right). \quad (13)$$

Similarly, two linear ranges obtained in the range of 2.0–10 µM and 15.0–50 µM for the DPV response were

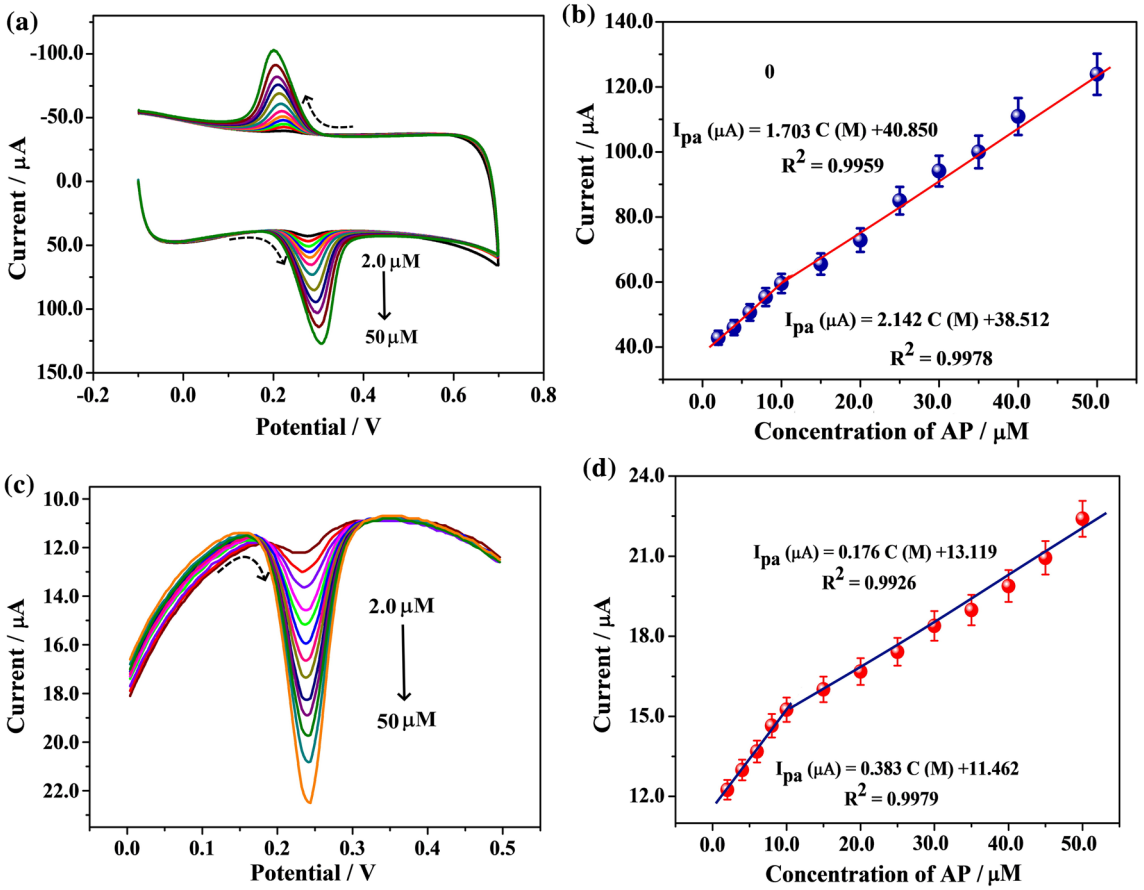

Fig. 8 (a) CVs for the various concentrations of AP from 2.0 µM to 50 µM in 0.2 M buffer solution (pH 7.0) at a scan rate of 0.1 V s^{-1} at the modified electrode, (b) Linear relationship between the CV response and the concentration of AP, (c) DPVs for various concentrations of AP from 2.0 µM to 50 µM in 0.2 M buffer solution (pH 7.0) at a scan rate of 0.1 V s^{-1} at the modified electrode, (d) The graph of peak current versus concentration of AP.

observed from Fig. 8d and the linear segment equations are displayed in the following Eqs. 14 and 15,

$$I_{pa}(\mu A)=11.462+0.383\ C\ (M)\ \left(R^2=0.9979\right) \quad (14)$$

$$I_{pa}(\mu A)=13.119+0.176\ C\ (M)\ \left(R^2=0.9926\right). \quad (15)$$

By considering the first linear ranges in both analytical curves of CV and DPV, the DL and QL were found from the following formula

$$\text{DL or QL}=k\times Sd/b \quad (16)$$

where $k = 10$ for QL and $k = 3$ for DL, Sd is the standard deviation of four blank signals, b is the slope of the analytical curve.[57] The obtained DL and QL via CV approach was 2.29×10^{-8} M and QL of 7.53×10^{-8} M, respectively. Using DPV, DL of 1.50×10^{-8} M and QL of 5.02×10^{-8} M was acquired. As apparent from the gained DL value, we can conclude that a lower DL value was achieved by DPV than CV. By considering the DPV approach, the figures of merit obtained for the analytical performance of the sensor were compared. The comparison is tabulated in Table I with the research papers that have been published to date and with their working electrode.[58–64] As inferred from Table I, the designed electrode exhibited a lower DL value compared to the other modified electrode revealing the efficiency of the CA/POAMCNTPE.

Reproducibility, Repeatability, Stability

To assess the reproducibility of the designed sensor, three separately prepared electrodes were subjected to CV measurement of 1×10^{-4} M of AP solution, and an RSD value of 3.9% was achieved from the reproducibility test. The value of RSD 2.8% was achieved for the repeatability of the sensor being tested by recording CVs with a different standard solution of 1×10^{-4} M AP and the same electrode. The lowest RSD value (below 4%) corresponding to repeatability and reproducibility renders the proposed electrode a good choice for the electroanalysis of AP. For stability study, CV scanning of 30 cycles was conducted for 1×10^{-4} M AP in a 0.2 M supporting electrolyte at CA/POAMCNTPE. A percentage degradation value of 3.8 was found from the following Eq. 17,

$$\%\text{degradation}=I_{pn}/I_{p1}\times100 \quad (17)$$

where I_{pn} and I_{p1} are the anodic peak current of the first and last cycle.[65] The obtained value confirms the stability of the developed sensor and shows that it does not undergo any surface fouling. Hence, the aforementioned outcomes shows the excellent stability, repeatability, and reproducibility of the developed sensor.

Selectivity Study

The selectivity study was intended to discover the impact of interfering biological compounds on the specificity measurement of AP using the designed sensor. To explore the sensor's selectivity, CV and DPV were employed to discover the capability of the sensor to detect AP in the presence of DA and FA, which co-exist with AP in the biological sample. CVs (Fig. 9a) and DPVs (Fig. 9c) depict the simultaneous detection of the 1×10^{-4} M AP, DA, and FA in the 0.2 M supporting electrolyte (pH 7.0) at CA/POAMCNTPE. As inferred from the CVs and DPVs, in the presence of DA and FA, anti-interference was observed in identifying AP, and simultaneous detection was possible in a mixture. In addition, DA and FA did not shift the voltammetric signal of AP and a large separation of oxidation peak was well observed. The above results show the selectivity of the developed sensor.

Table I Analytical features of the proposed CV method using the adopted sensor compared to the data of other voltammetric methods applied to detect the AP.

Serial No.	Electrodes	Linear working range of AP (μM)	Detection limit of AP (μM)	References
1.	HNED–MWCNTPE	100–1400	0.046	58
2.	PMG/fMWCNT/GCE	25–200	4.3	59
3.	MWCNT/TiO_2/GCE	10–120	11.77	60
4.	ZY/SDS/MSPE	0.4–100	0.080	61
5.	CPBMWCNT	5.0–92.6	0.57	62
6.	4ABSA/GCE	0.6–90	0.093	63
7.	Au/Pd/rGO	1.0–250	0.30	64
8.	CA/POAMCNTPE	2.0–50	0.015	Present work

HNED N,N-bis-(2-hydroxy-1-naphthalidene)ethylenediamine, *PMG/f-MWCNT* Poly(methylene green) functional multi-walled carbon nanotubes, *GCE* Glassy carbon electrode, *TiO_2* Titanium dioxide, *ZY/SDS/MSPE* Zeolite bulk-modified screen printed electrode, *CPB* Cetypyridinum bromide, *Au/Pd/rGo* Palladium-reduced graphene oxide, *4-ABSA* 4-aminobenzene sulfonic acid.

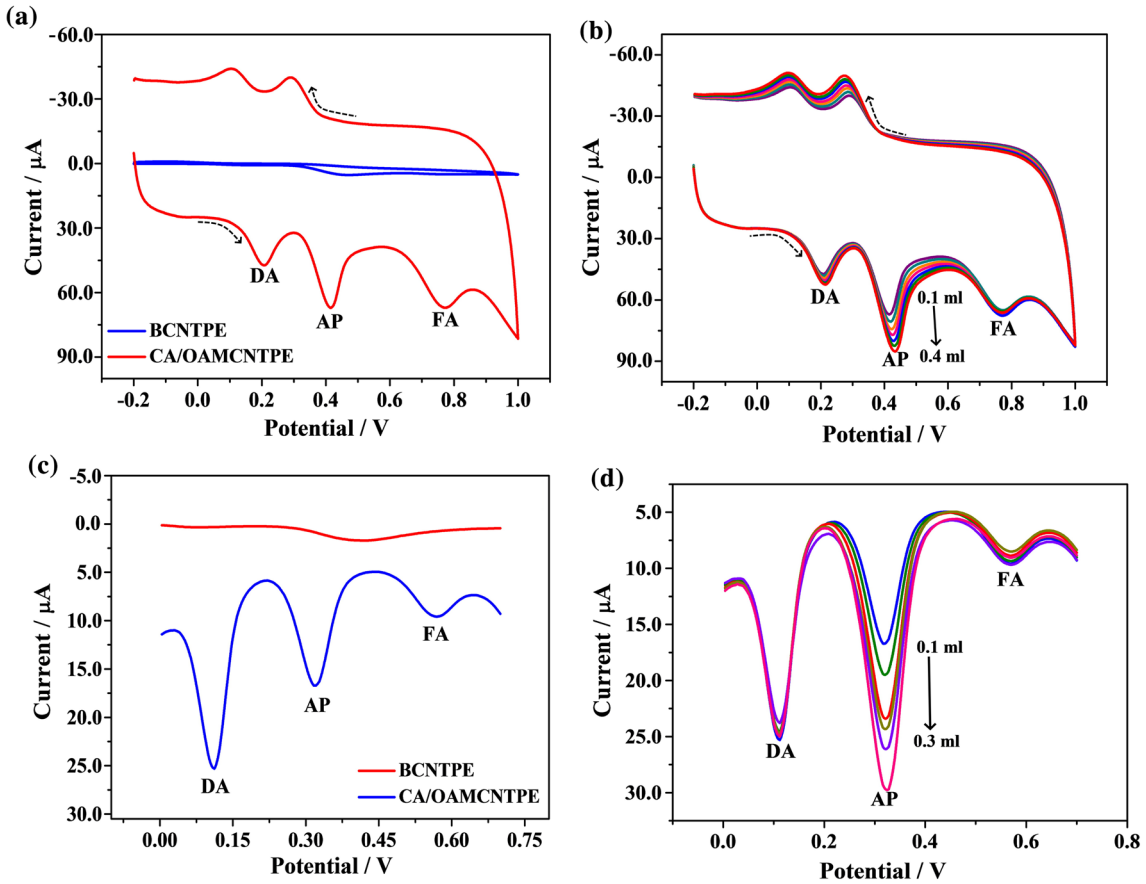

Fig. 9 (a) CVs of the 1×10^{-4} M AP, DA and FA mixture in the supporting electrolyte (pH 7.0) at 0.1 V s^{-1} scan rate using CA/POAMCNTPE and BCNTPE, (b) CVs for increasing the concentration of AP from 1.0×10^{-4} M to 4.0×10^{-4} M by keeping the concentration of FA and DA constant, (c) DPVs of the 1×10^{-4} M AP, DA and FA mixture in the supporting electrolyte (pH 7.0) at a scan rate of 0.1 V s^{-1} using CA/POAMCNTPE and BCNTPE, (d) DPVs for increasing the concentration of AP from 1.0×10^{-4} M to 3.5×10^{-4} M by keeping the concentration of FA and DA constant.

The interference study was further extended by increasing the concentration of AP from 1.0×10^{-4} M to 4.0×10^{-4} M and keeping DA and FA concentration constant in the 0.2 M supporting electrolyte (pH 7.0) at a sweep rate of 0.1 V s^{-1} by CV and DPV. The corresponding CVs and DPVs are depicted in Fig. 9b, d, respectively. As can be seen from the figure, the magnitude of the peak increased with the increasing concentration of AP, but DA and FA still have an unchanged current response in both the CV and DPV. This proves that the designed sensor has an outstanding specificity towards the detection of AP in the presence of DA and FA.

Real Sample Analysis

To understand the feasibility of the fabricated sensor it was employed to sense the AP in a real sample. The real sample analysis was performed in a pharmaceutical and biological sample such as a blood serum sample. A tablet containing AP was procured from local a pharmacy. An AP tablet solution prepared from the powdered tablet was obtained for CV measurement. The obtained outcomes are listed in Table II. A good recovery between 98% and 101% was acquired from the developed method. More importantly, the practicability of the sensor was also evaluated in the blood serum samples. The blood serum sample was directly taken for measurement

Table II Recovery studies for the electroanalysis of the AP in the tablet sample using the proposed method.

Pharmaceutical sample	Concentration added (µM)	Found value (µM)	Recovery (%)
Sample 1	40	41.2	103
	60	59.8	99.6
	80	80.2	101.2
Sample 2	40	40.5	101.2
	60	60.8	101.3
	80	79.2	99

Table III Recovery studies for the electroanalysis of AP in the blood serum sample using the proposed electrode.

Biological sample	Concentration added (μM)	Found value (μM)	Recovery (%)
Blood serum sample	30	31.2	100.6
	60	59.6	99.3
	90	90.8	100.8

by the spiked method. The obtained results are presented in Table III showing a satisfactory recovery. These results show that the developed method is appropriate for routine analysis.

Conclusion

The electrochemical sensor developed based on the CA/POAMCNTPE to detect the AP via CV and DPV was introduced in this work. The electrochemical reaction of AP on the surface showed an excellent current response and quasi-reversible redox processes compared to the bare electrode. The topographical features of BCNTPE and CA/POAMCNTPE were demonstrated via VP-SEM. The electrochemical characterisation of the prepared sensor was evaluated by utilising K_4 [Fe (CN_6)] as the redox probe. The resistivity of the proposed electrode was studied through EIS analysis. The modified electrode possesses a higher surface-active area than the unmodified electrode. The redox reaction of AP at the modified electrode was pH-dependent and the reaction resulted in losing two electrons. The ratio of the number of transferred electrons and protons was calculated. The pH condition was optimised and scan rate studies reveal that the redox behaviour of AP at the modified electrode was controlled by diffusion. The number of transferred electrons during the electroanalysis was estimated as two. The analytical curve of AP at the sensor yielded the desired low DL value through DPV. The selectivity of the designed electrode was explored in presence of DA and FA. The modified electrode has anti-interference, reproducibility, repeatability and anti-fouling properties. Therefore, a designed sensor was successfully employed for the significant detection of AP in tablets and in blood serum samples. Hence, the developed sensor is an appropriate candidate for the regular assessment of AP.

Acknowledgments We gratefully acknowledge the financial support from the SC/ST Fellowship No. MU/SCT RF/CR17/2017-18 Mangalore University.

Conflict of interest The authors confirm they have no conflict of interest.

References

1. A. Kassa, and M. Amare, *Cogent Chem.* 5, 1 (2019). https://doi.org/10.1080/23312009.2019.1681607.
2. J.L. Stringer, *Basic Concepts in Pharmacology: What You Need to Know for Each Drug Class*, 5th ed., (Mc Graw-Hill Professional, 2017).
3. F. Ellis, *Paracetamol—A Curriculum Resource* (London: Royal Society of Chemistry, 2002).
4. W.H. Martindale, *The Extra Pharmacopoeia*, 29th ed., (London: The Pharmaceutical Press, 1989), p. 32.
5. R. Chokkareddy, N. Thondavada, N.K. Bhajanthri, and G.G. Redhi, *Anal. Methods.* 11, 6204 (2019). https://doi.org/10.1039/c9ay01743g.
6. R.T. Kachoosangi, G.G. Wildgoose, and R.G. Compton, *Analytica chim. Acta.* 618, 54 (2008). https://doi.org/10.1016/j.aca.2008.04.053.
7. B. Habibi, M. Jahanbakhshi, and M.H. Pournaghi-Azar, *Electrochim. Acta.* 56, 2888 (2011). https://doi.org/10.1016/j.electacta.2010.12.079.
8. M.T. Olaleye, and B.J. Rocha, *Exp. Toxicol. Pathol.* 59, 319 (2008). https://doi.org/10.1016/j.etp.2007.10.003.
9. M. Mazer, and J. Perrone, *J. Med. Toxicol.* 4, 2 (2008). https://doi.org/10.1007/bf03160941.
10. E. Hazai, L. Vereczkey, and K. Monostory, *Biochem. Biophys. Res. Commun.* 291, 1089 (2002). https://doi.org/10.1006/bbrc.2002.6541.
11. M.E. Bosch, A.J.R. Sanchez, F.S. Rojas, and C.B. Ojeda, *J. Pharm. Biomed. Anal.* 42, 291 (2006). https://doi.org/10.1016/j.jpba.2006.04.007.
12. S. Zhao, W. Bai, H. Yuan, and D. Xiao, *Anal. Chim. Acta.* 559, 195 (2006). https://doi.org/10.1016/j.aca.2005.11.071.
13. W. Ruengsitagoon, S. Liawruangrath, and A. Townshend, *Talanta* 69, 976 (2006). https://doi.org/10.1016/j.talanta.2005.11.050.
14. I. Baranowska, and B. Kowalski, *Water Air Soil Pollut.* 211, 417 (2010). https://doi.org/10.1007/s11270-009-0310-7.
15. G.M. Hadad, S. Emara, and W.M.M. Mahmoud, *Talanta* 79, 1360 (2009). https://doi.org/10.1016/j.talanta.2009.06.003.
16. N. Al-Zhoubi, J.E. Koundourellis, and S. Malamataris, *J. Pharm. Biomed. Anal.* 29, 459 (2002). https://doi.org/10.1016/S0731-7085(02)00098-5.
17. M.S.M. Quintino, K. Araki, H.E. Toma, and L. Angnes, *Electroanalysis* 14, 1629 (2002). https://doi.org/10.1002/elan.200290003.
18. M.G. Gioia, P. Andreatta, S. Boschetti, and R. Gatti, *J. Pharm. Biomed. Anal.* 48, 331 (2008). https://doi.org/10.1016/j.jpba.2008.01.026.
19. W. Lohmann, and U. Karst, *Anal. Bioanal. Chem.* 386, 1701 (2006). https://doi.org/10.1007/s00216-006-0801-y.
20. H.G. Lou, H. Yuan, Z.R. Ruan, and B. Jiang, *J. Chromatogr. B.* 878, 682 (2010). https://doi.org/10.1016/j.jchromb.2010.01.005.
21. M.K. Srivastava, S. Ahmad, D. Singh, and I.C. Shukla, *Analyst.* 110, 735 (1985). https://doi.org/10.1039/AN9851000735.
22. G. Burgot, F. Auffret, and J.L. Burgot, *Anal. Chim. Acta.* 343, 125 (1997). https://doi.org/10.1016/s0003-2670(96)00613-7.
23. Y.Z. Fang, D.J. Long, and J.N. Ye, *Anal. Chim. Acta.* 342, 13 (1997). https://doi.org/10.1016/S0003-2670(96)00619-8.
24. A.R. Khaskheli, A. Shah, M.I. Bhanger, A. Niaz, and S. Mahesar, *Spectrochim. Acta A Mol. Biomol. Spectrosc.* 68, 747 (2007). https://doi.org/10.1016/j.saa.2006.12.055.
25. H.M. Moghaddam, H. Beitollahi, S. Tajik, S. Jahani, H. Khabazzadeh, and R. Alizadeh, *Russ. J. Electrochem.* 53, 452 (2017). https://doi.org/10.1134/s1023193517050123.
26. S. Tajik, Z. Dourandish, K. Zhang, H. Beitollahi, Q. Van Le, H.W. Jang, and M. Shokouhimehr, *RSC Adv.* 10, 15406 (2020). https://doi.org/10.1039/d0ra00799d.

27. H.M. Moghaddam, S. Tajik, and H. Beitollahi, *Microchem. J.* 150, 104085 (2019). https://doi.org/10.1016/j.microc.2019.104085.
28. H. Beitollahi, M.A. Khalilzadeh, S. Tajik, M. Safaei, K. Zhang, H.W. Jang, and M. Shokouhimehr, *ACS Omega* (2020). https://doi.org/10.1021/acsomega.9b03788.
29. H. Beitollahi, H.M. Moghaddam, and S. Tajik, *Anal. Lett.* (2018). https://doi.org/10.1080/00032719.2018.1545132.
30. H. Karimi-Maleh, M. Alizadeh, Y. Orooji, F. Karimi, M. Baghayeri, J. Rouhi, S. Tajik, H. Beitollahi, S. Agarwal, V.K. Gupta, S. Rajendran, S. Rostamnia, L. Fu, F. Saberi-Movahed, and S. Malekmohammadi, *Ind. Eng. Chem. Res.* 60, 816 (2021). https://doi.org/10.1021/acs.iecr.0c04698.
31. F.G. Nejad, S. Tajik, H. Beitollahi, and I. Sheikhshoaie, *Talanta* 228, 122075 (2021).
32. S. Tajik, H. Beitollahi, F.G. Nejad, Z. Dourandish, M.A. Khalilzadeh, H.W. Jang, R.A. Venditti, R.S. Varma, and M. Shokouhimehr, *Ind. Eng. Chem. Res.* 60, 1112 (2021). https://doi.org/10.1021/acs.iecr.0c04952.
33. S. Tajik, H. Beitollahi, H.W. Jang, and M. Shokouhimehr, *Talanta* 232, 122379 (2021). https://doi.org/10.1016/j.talanta.2021.122379.
34. H. Karimi-Maleh, Y. Orooji, F. Karimi, M. Alizadeh, M. Baghayeri, J. Rouchi, S. Tajik, H. Beitollahi, S. Agarwal, V.K. Gupta, S. Rajendran, A. Ayati, L. Fu, A.L. Sanati, B. Tanhaei, F. Sen, M. Nooshabadi, P.N. Asrami, and A. Othman, *Biosens. Bioelectron.* 184, 113252 (2021). https://doi.org/10.1016/j.bios.2021.113252.
35. J.G. Manjunatha, *Int. J. ChemTech Res.* 6, 136 (2016).
36. H. Karimi-Maleh, F. Karimi, Y. Orooji, G. Mansouri, A. Razmjou, A. Aygun, and F. Sen, *Sci. Rep.* 10, 1 (2020). https://doi.org/10.1038/s41598-020-68663-2.
37. M.M. Charithra, and J.G. Manjunatha, *J. Electrochem. Sci. Eng.* 10, 29 (2020). https://doi.org/10.5599/jese.717.
38. J.G. Manjunatha, B.E. Kumara Swamy, M.T. Shreenivas, and G.P. Mamatha, *Anal. Bioanal. Electrochem.* 4, 225 (2012).
39. J.G. Manjunatha, M. Deraman, and N.H. Basri, *Asian J. Pharm. Clin. Res.* 8, 48 (2015).
40. H. Zhu, X. Wang, J. Liang, H. Lv, H. Tong, L. Ma, Y. Hu, G. Zhu, T. Zhang, Z. Tie, Z. Liu, Q. Li, L. Chen, J. Liu, and Z. Jin, *Adv. Funct. Mater.* 27, 1606604 (2017). https://doi.org/10.1002/adfm.201606604.
41. B. Yoon, S.F. Liu, and T.M. Swager, *Chem Mater.* 28, 5916 (2016). https://doi.org/10.1021/acs.chemmater.6b02453.
42. L. Li, P. Shi, L. Hua, J. An, Y. Gong, R. Chen, C. Yu, W. Hua, F. Xiu, J. Zhou, G. Gao, Z. Jin, G. Sun, and W. Huang, *Nanoscale* 10, 118 (2018). https://doi.org/10.1039/c7nr06219b.
43. H. Luo, Z. Shi, N. Li, Z. Gu, and Q. Zhuang, *Anal. Chem.* 73, 915 (2001). https://doi.org/10.1021/ac000967l.
44. C.P. Jonesa, K. Jurkschat, A. Crossley, and C.E. Banks, *J. Iran. Chem. Soc.* 5, 279 (2008). https://doi.org/10.1007/BF03246119.
45. H. Karimi-Maleh, A.F. Shojaei, F. Karimi, K. Tabatabaeian, S. Shakeri, and R. Moradi, *Biosens. Bioelectron.* 86, 879 (2016). https://doi.org/10.1016/j.bios.2016.07.086.
46. R.R. Moore, C.E. Banks, and R.G. Compton, *Anal. Chem.* 76, 2677 (2004). https://doi.org/10.1021/ac040017q.
47. M. Ates, *Mater. Sci. Eng.* 33, 1853 (2013). https://doi.org/10.1016/j.msec.2013.01.035.
48. J.G. Manjunatha, *J. Electrochem. Sci. Eng.* 7, 39 (2017). https://doi.org/10.5599/jese.368.
49. M.M. Charithra, J.G. Manjunatha, and C. Raril, *Adv. Pharm. Bull.* 10, 247 (2020). https://doi.org/10.34172/apb.2020.029.
50. J.G. Manjunatha, and G.K. Jayaprakash, *Euarasian J. Anal. Chem.* 14, 1 (2019). https://doi.org/10.29333/ejac/20190101.
51. V. Prabhakara Rao, Y. Veera Manohara Reddy, M. Lavanya, M. Venu, and G. Madavi, *Asian J. Chem.* 28, 1828 (2016). https://doi.org/10.14233/ajchem.2016.19877.
52. M.M. Charithra, and J.G. Manjunatha, *ChemistrySelect* 5, 9323 (2020). https://doi.org/10.1002/slct.202002626.
53. P.K. Kalambate, B.J. Sanghavi, S.P. Karna, and A.K. Srivastava, *Sens. Actuators B Chem.* 213, 285 (2015). https://doi.org/10.1016/j.snb.2015.02.090.
54. A.U. Alam, Y. Qin, M.M.R. Howlader, N.-X. Hu, and M. Jamal Deen, *Sens. Actuators B.* 254, 896 (2018). https://doi.org/10.1016/j.snb.2017.07.127.
55. M. Amare, *Heliyon* 5, 1 (2019). https://doi.org/10.1016/j.heliyon.2019.e01663.
56. M.M. Charithra, and J.G. Manjunatha, *Mater. Chem. Phys.* 262, 124293 (2021). https://doi.org/10.1016/j.matchemphys.2021.124293.
57. J. Mocak, A. Bond, S. Mitchell, and G. Scollary, *Pure Appl. Chem.* 69, 297 (1997). https://doi.org/10.1351/pac199769020297.
58. M. Behpour, S. Ghoreishi, M. Meshki, and H. Naemi, *J. Anal. Chem.* 69, 982 (2014). https://doi.org/10.1134/S1061934814100098.
59. M.M. Barsan, C.T. Toledo, and C.M. Brett, *J. Electroanal. Chem.* 736, 8 (2015). https://doi.org/10.1016/j.jelechem.2014.10.026.
60. A.A. Pasban, E.H. Nia, and M. Piryaei, *J. Nanoanal.* 4, 142 (2017). https://doi.org/10.22034/jna.2017.02.007.
61. S.A. Atty, A.H. Ibrahim, and E.M. Hussien, *J. Electrochem. Soc.* 166, B1483 (2019). https://doi.org/10.1149/2.0961914jes.
62. F.F. Hudari, E.H. Duarte, A.C. Pereira, L.H. Dall'Antonia, L.T. Kubota, and C.R.T. Tarley, *J. Electroanal. Chem.* 696, 52 (2013). https://doi.org/10.1016/j.jelechem.2013.01.033.
63. S. Yilmaz, Z. Bas, M. Sadikoglu, S. Yagmur, and G. Saglikoglu, *Int. J. Electrochem. Sci.* 11, 6244 (2016). https://doi.org/10.20964/2016.07.74.
64. H. Wang, S. Zhang, S. Li, and J. Qu, *Talanta* 178, 188 (2018). https://doi.org/10.1016/j.talanta.2017.09.021.
65. C. Raril, and J.G. Manjunatha, *Mod. Chem. Appl.* 6, 1 (2018). https://doi.org/10.4172/2329-6798.1000263.